

RESEARCH

Open Access



Distal airway stem cells ameliorate bleomycin-induced pulmonary fibrosis in mice

Yun Shi^{1†}, Mingqing Dong^{2†}, Yueqing Zhou^{3,4†}, Wangping Li¹, Yongheng Gao¹, Luyao Han¹, Min Chen¹, Hongwei Lin¹, Wei Zuo^{3,4,5*} and Faguang Jin^{1*}

Abstract

Background: Idiopathic pulmonary fibrosis is characterized by loss of lung epithelial cells and inexorable progression of fibrosis with no effective and approved treatments. The distal airway stem/progenitor cells (DASCs) have been shown to have potent regenerative capacity after lung injury. In this work, we aimed to define the role of mouse DASCs (mDASCs) in response to bleomycin-induced lung fibrosis in mice.

Methods: The mDASCs were isolated, expanded in vitro, and labeled with GFP by lentiviral infection. The labeled mDASCs were intratracheally instilled into bleomycin-induced pulmonary fibrosis mice on day 7. Pathological change, collagen content, α -SMA expression, lung function, and mortality rate were assessed at 7, 14, and 21 days after bleomycin administration. Tissue section and direct fluorescence staining was used to show the distribution and differentiation of mDASCs in lung.

Results: The transplanted mDASCs could incorporate, proliferate, and differentiate into type I pneumocytes in bleomycin-injured lung. They also inhibited fibrogenesis by attenuating the deposition of collagen and expression of α -SMA. In addition, mDASCs improved pulmonary function and reduce mortality in bleomycin-induced pulmonary fibrosis mice.

Conclusions: The data strongly suggest that mDASCs could ameliorate bleomycin-induced pulmonary fibrosis by promotion of lung regeneration and inhibition of lung fibrogenesis.

Keywords: Pulmonary fibrosis, Distal airway stem/progenitor cells, Bleomycin

Background

Idiopathic pulmonary fibrosis (IPF) is an idiopathic interstitial lung disease characterized by loss of lung epithelial cells and inexorable progression of fibrosis, which results in loss of normal lung architecture, respiratory failure, and eventual fatal outcome [1–3]. Currently, there is no effective therapy for pulmonary fibrosis for lack of known etiology and adequate knowledge of their pathogenic mechanisms [4]. Therefore, there is an

urgent need for developing new methods for the treatment of IPF [5].

Recently, interest has accumulated regarding tissue regeneration as a new therapeutic strategy for lung fibrosis. Broadly, tissue regeneration is achieved by proliferation of common differentiated cells and/or by deployment of specialized stem/progenitor cells, which has been applied in some studies [6–10]. After lung damage, adult lung tissue has a remarkable capacity for regeneration, owing to a few facultative stem/progenitor cell populations that become activated in response to tissue damage [11, 12]. The distal airway stem/progenitor cells (DASCs) expressing basal cell-restricted transcription factor p63 and keratin-5 (KRT5) have been shown to have potent regenerative capacity after lung injury [13–16]. Influenza-induced lung injury activated DASCs to proliferate and

* Correspondence: zuow@tongji.edu.cn; jinfag@fmmu.edu.cn

[†]Yun Shi, Mingqing Dong and Yueqing Zhou contributed equally to this work.

³Shanghai East Hospital, School of Medicine, Tongji University, Shanghai 200120, People's Republic of China

¹Department of Respiratory and Critical Care Medicine, Tangdu Hospital, Fourth Military Medical University, Xi'an 710038, People's Republic of China
Full list of author information is available at the end of the article



migrate widely to occupy heavily injured areas, whereupon they differentiate toward mature epithelium and the regeneration of injured tissue depending on the extent of injury [14]. The feasibility for large-scale *in vitro* expansion and remarkable lung engraftment after transplantation make DASC an ideal candidate for cell therapy [15, 17].

In the current study, we aim to determine whether mouse DASC (mDASC) transplant has protective effects against bleomycin-induced lung fibrosis in mice. The results showed that mDASCs could incorporate, proliferate, and differentiate into type I pneumocytes. In addition, mDASCs could inhibit pulmonary fibrogenesis by attenuating the deposition of collagen and the expression of α -SMA in lungs. Furthermore, mDASCs improved the pulmonary function and reduced the animal's mortality in bleomycin-induced pulmonary fibrosis mice. The results indicated that DASCs may be an ideal candidate for the cell therapy of pulmonary fibrosis.

Methods

Isolation and culture of mDASCs

The isolation and culture of mDASCs was based on previously described methods [15]. Briefly, the lung tissue of adult mice was collected and immersed in cold wash buffer (F12 medium, 1% Pen/Strep, 5% FBS). The trachea and two main bronchi were separated from the lungs, and the lobes were cut with a sterile surgical blade into small pieces and digested with dissociation buffer (F12/DMEM, 1 mg/mL protease, 0.005% trypsin and 10 ng/mL DNaseI) overnight with gentle rocking. Dissociated cells were passed through 70- μ m Nylon mesh, washed with cold F12 medium, and then plated onto irradiated 3T3 feeder cells as described. Under 7.5% CO₂ culture condition, the mDASC colonies emerged 3–5 days after plating. Cells were digested by 0.25% trypsin-EDTA (Gibco, USA) for 3–5 min for passaging. To label cells with GFP, pLenti-CMV-EGFP plasmid was transfected into 293T cells together with lentiviral packaging mix (Life Technologies, USA). Lentivirus supernatant produced by 293T was collected, filtered, and cryo-preserved before use. To infect mDASCs, 0.5 mL lentivirus containing medium was directly added to 2 mL cell culture medium with 10 μ g/mL polybrene and incubated for 12 h, and the overall labeling efficiency of cells was above 95%.

Differentiation of mDASCs *in vitro*

The mDASCs were seeded on Matrigel Matrix (Corning, USA) as previously described [13]. Cells were cultured in serum-free DMEM/F12 medium for 7 days, adding FGF10 (50 ng/mL, Peprotech, USA), transferrin (5 μ g/mL, Peprotech, USA), HGF (20 ng/mL, Peprotech, USA), 2% Matrigel, and 5% BSA. Differentiated organoids were harvested and embedded in Tissue-Tek O.C.T. Compound (Sakura,

USA), then the differentiation characteristics of cells were identified by immunofluorescence.

Mice, bleomycin injury models, and treatment protocols

Six- to 8-week-old female C57/B6 mice were purchased from Vital River (China) and were housed in the SPF animal facility. All studies were approved by the Institutional Animal Care and Use Committee of the Fourth Military Medical University. Mice were anesthetized with isoflurane, the lung was injured by intratracheally instilling with 3 U/kg bleomycin (Selleckchem, USA) in the volume of 30 μ l on day 0, and the weight of the mice was recorded 7, 14, and 21 days after injury. One million GFP-labeled mDASCs in a volume of 30 μ l or saline were transplanted on day 7 after injury. Intratracheal aspiration was performed by injecting the cells into the trachea via the mouth which was described in our previous publications [15]. The mDASCs were counted, washed, and resuspended by PBS before transplantation. Bright-field and direct fluorescence of the transplanted lung were acquired under the fluorescence stereomicroscope (MVX10, Olympus, Japan).

Lung wet-to-dry weight (W/D) ratios

To quantify the magnitude of pulmonary edema caused by bleomycin, we evaluated the wet-to-dry ratios. The lungs were excised at an indicated day after injury, and the wet weight was recorded. The dry weights were obtained after the lungs were dried in an oven at 70 °C for 72 h. The W/D ratios were then calculated.

Tissue histology

At appropriate time points, mice were euthanized and the diaphragm was carefully cut open without touching the lung. The lung was inflated with 3.7% formaldehyde (Sigma, USA) using a 30-G needle through the trachea. Then the lung was dissected and fixed in 3.7% formaldehyde at 4 °C overnight before paraffin section or cryosection. For cryosection, the fixed lung was settled by 30% sucrose before embedding into the Tissue-Tek O.C.T compound (Sakura, Japan), solidified on dry ice, and cut using a cryotome (Leica Microsystems, Germany) of 5–10- μ m thickness. For the paraffin section, the lung was dehydrated by gradient ethanol in an automatic tissue processor (Leica Microsystems, Germany) and then embedded into paraffin blocks. The blocks were cut into 5–7- μ m thickness by using a microtome (Leica Microsystems, Germany) at distinct planes. The sections were placed on poly-lysine-coated glass slides and stored at room temperature until further use. Hematoxylin and eosin (H&E) and Masson's trichrome staining was performed following the standard protocol. The severity of fibrosis in H&E-stained lungs was quantified by the Ashcroft scoring system [18], and the blue-stained area

(an indication of quantity of collagen deposition) was separately quantified by ImageJ version 1.52a (National Institutes of Health, USA).

Immunofluorescence staining

For immunofluorescence staining, cryo-embedded tissue slides were subjected to antigen retrieval in citrate buffer (pH 6, Sigma-Aldrich, USA) at 120 °C for 20 min, and 10% normal donkey serum (Jackson Immuno Research) was used to block the non-specific antigen. Antibodies used for immunofluorescence included mDASC markers: KRT5 (1:200, ab128190, Abcam) and P63 (deltaN, 1:200, 4A4, Abcam); pneumocyte markers: PDPN (1:200, FL-162, Santa Cruz), AQP5 (1:200, EPR3747, Abcam), and HOPX (1:200, E-1, Santa Cruz); myofibroblast marker: α -SMA (1:500, 1A4, DAKO); and others: GFP (1:1000, ab5450, Abcam) and KI67 (1:200, RM-9106, Thermo). Alexa Fluor-conjugated Donkey 488/594/647 (1:200, Life Technologies, USA) were used as secondary antibodies. After counter staining with DAPI (Roche, USA), samples were treated with 0.1% Sudan Black (Sigma, USA) for 1–2 min to remove autofluorescence and then mounted with VECTASHIELD® Mounting medium (Vector Labs, USA). Stained slides were stored at 4 °C in the dark, and images were taken by using a fluorescence microscope (Nikon 80i and Eclipse Ti, Nikon, Japan).

Measurement of lung hydroxyproline

To evaluate the extent of tissue fibrosis, we measured the total collagen contents using a hydroxyproline assay kit (Nanjing Jiancheng Bioengineering Institute, China). The experimental procedure was according to the manufacturer's instructions.

Western blotting

The tissues were collected and homogenized immediately, and the protein was extracted using the Total Protein Extraction Kit. The BCA protein assay kit was used to determine the protein concentration. Twenty micrograms total protein was loaded and separated on a 10% SDS poly-acrylamide gel, and then transferred to the PVDF membrane (Roche). The membrane was blocked with 5% non-fat dry milk for 2 h, followed by incubation with primary antibodies against α -SMA (1:500, 1A4, DAKO) or GAPDH (1:500, GB12002, Servicebio) overnight. Then the membrane was incubated with the secondary antibody. The specific signals were detected by the Immobilon Western Chemiluminescent HRP Substrate (Millipore) and Tanon image system.

Arterial blood gas measurements

Mice were anesthetized at appropriate time points, and the blood samples were drawn from the carotid aorta into polypropylene syringes containing 60 IU of dry,

electrolyte-balanced heparin (PICO70; Radiometer Medical, Copenhagen, Denmark). The partial oxygen pressure (pO₂), partial carbon dioxide pressure (pCO₂), and oxygen saturation (sO₂) were measured using an ABL90 Flex Blood Gas Analyzer (Radiometer Medical). Independent DASC isolations were used, and the engraftment levels of GFP-mDASC were evaluated under a stereo fluorescence microscope. Only the animals with similar levels of engraftment of GFP-mDASC were used for analysis.

Survival studies

For the assessment of mortality rates, mice were given 5 U/kg bleomycin by intratracheal aspiration on day 0 and transplanted by mDASCs or saline on day 7. The mortality of mice in each group was recorded every day for 24 days after bleomycin administration.

Statistics

Statistical calculations were performed using GraphPad Prism (GraphPad Software, Inc., San Diego, CA, USA). Comparisons between two groups were made by an unpaired *t* test. Comparisons between more than two groups were analyzed by one-way ANOVA or two-way ANOVA with post Tukey's multiple comparisons test. Survival data were presented by the Kaplan–Meier method, and comparisons were made by the log rank test. All values were expressed as means \pm SEM. **P* < 0.05 and ***P* < 0.01 were considered statistically significant.

Results

Characterization of endogenous mDASCs in bleomycin-induced lung injury in mice

Delivery of bleomycin to the lung caused acute pulmonary injury that was mirrored by the changes of weight and wet/dry ratios. The weight of pulmonary injury model mouse decreased, but the weight of control mouse increased significantly during the experiment (Fig. 1a). The weight was significantly different between the control mouse and model mouse at 7, 14, and 21 days after bleomycin delivery (all *P* < 0.05, *n* = 3). The lung wet/dry ratios of the injury mouse significantly increased 7, 14, and 21 days after bleomycin administration compared with those of the control mouse (all *P* < 0.05, *n* = 3) (Fig. 1b).

It had been demonstrated that the expression of KRT5 and P63 was the characteristic marker of distal airway stem cells; we found little evidence of KRT5+P63+ cells in the parenchyma of normal mice. However, 7 days after administration of bleomycin, some KRT5+P63+ cells could be found in the bronchioles by immunofluorescence; these cells in the damage lung appeared to cluster in small groups and are distributed in a concentric pattern about the bronchioles, and these cells also could

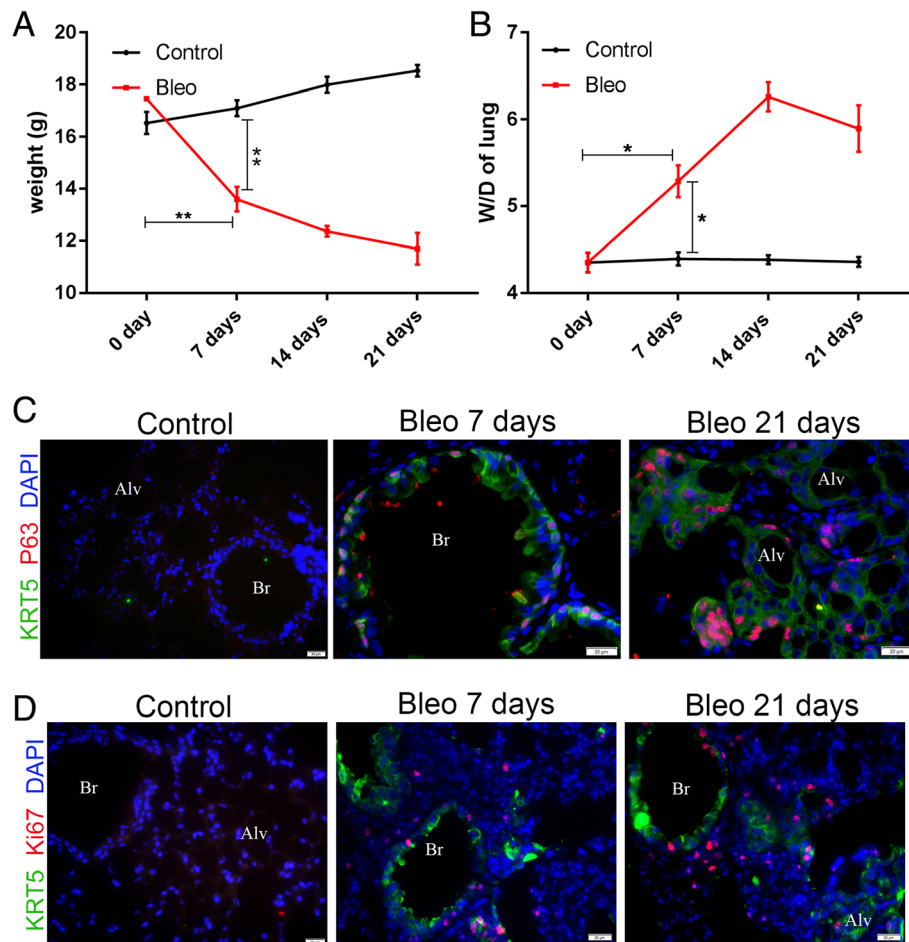


Fig. 1 Characterization of endogenous mDASCs in bleomycin-induced lung injury in mice. **a** The weight changes of mice after the delivery of bleomycin. $n = 3$. Error bars, S.E.M. $**P < 0.01$. **b** The lung wet-to-dry weight ratios induced by bleomycin. $n = 3$. Error bars, S.E.M. $*P < 0.05$. **c** Anti-KRT5 and anti-P63 immunofluorescence staining of a lung section 7 and 21 days after administration of bleomycin. **d** Anti-KRT5 and anti-Ki67 immunofluorescence staining of a lung section 7 and 21 days after administration of bleomycin. Br, bronchioles; Alv, alveoli. Scale bar, 20 μ m

be found in broader regions of the alveolar space as time went on (Fig. 1c, Additional file 1: Figure S1a and b). A fraction of these cells expressed proliferation marker Ki67 (Fig. 1d and Additional file 1: Figure S1c), suggesting their high viability and extended contribution to the repair process.

Transplanted mDASCs incorporated in damaged lung and differentiated into type I pneumocytes

Although the endogenous KRT5+P63+ cells could be found in broader regions of the alveolar space as time went on, their number was still less and not enough to inhibit the progression of bleomycin-induced fibrosis (Additional file 2: Figure S2a). Therefore, we investigated the effect of exogenous mDASCs by transplanting them into the lungs of bleomycin-injured mice.

To make sure that the transplanted cells were DASCs but not just other basal cells, which also express P63 and Krt5, the transplanted mDASCs were identified by

culturing in Matrigel. The mDASCs expressed the markers of P63 and KRT5 (Fig. 2a), which formed an alveolar-like sphere structure with the type I alveolar cell marker AQP5 expression during a 7-day period of culture (Fig. 2b), which was consistent with previous studies [15].

Then, we investigated the effect of mDASCs by isolating, culturing, and transplanting them into the lung of mice. One million GFP-labeled mDASCs were transplanted into the lung 7 days after bleomycin injury. The tissues were harvested for analysis on 7 and 14 days after cell transplantation (Fig. 2c). Substantial incorporation of mDASCs (and their descendants) into mouse lung was detected along the days (Fig. 2d). Direct fluorescence of tissue section showed distribution of GFP-mDASCs in mouse lung parenchyma, and a fraction of mDASCs differentiated into an alveolar-like structure in later days (Fig. 3a). Expectedly, we observed the incorporation of mDASCs with expression of KRT5 and P63 7

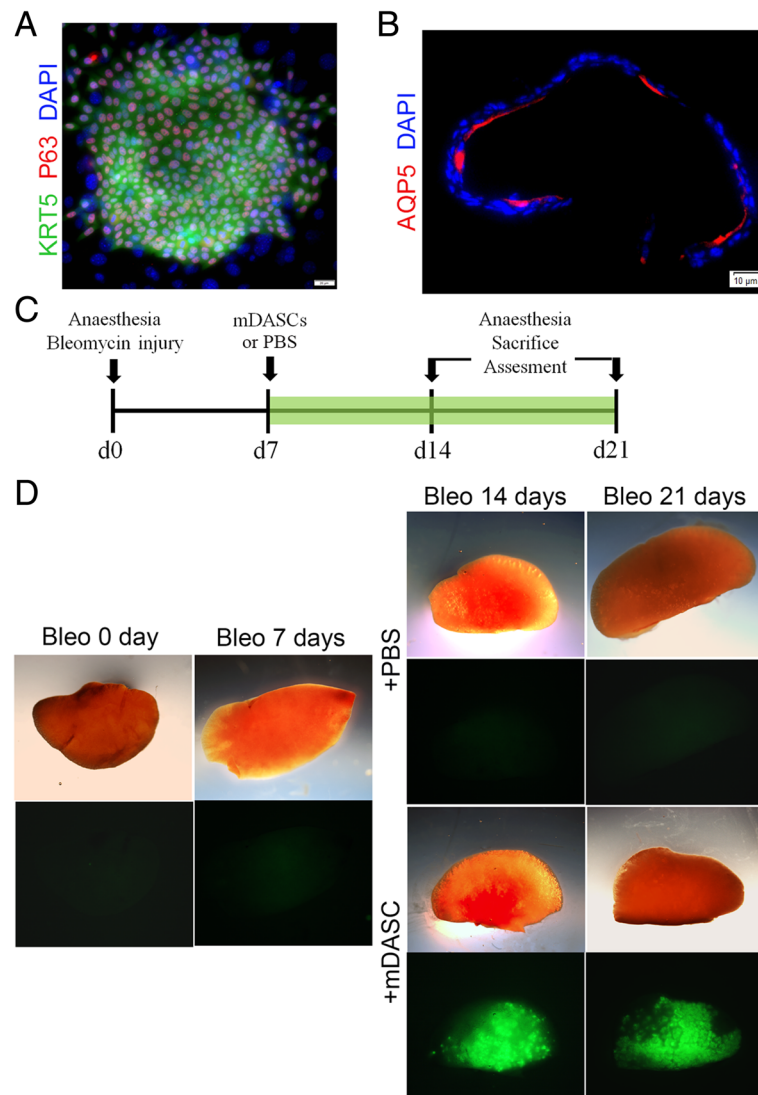


Fig. 2 The mDASCs differentiated into type I pneumocytes in vitro and incorporated in damaged lung. **a** Anti-KRT5 and anti-P63 immunostaining of mDASC colonies with nuclei counterstain. Scale bar, 20 μ m. **b** Differentiation of mDASCs in three-dimensional Matrigel cultures showing an alveolar-like sphere structure and expression of AQP5 (type I alveolar cell marker). Scale bar, 10 μ m. **c** Schematic diagram of the experiment. **d** Bright-field and direct fluorescence image of mouse lungs following transplantation of 1×10^5 GFP-labeled mDASCs on the indicated days after bleomycin injury

days after transplantation (Fig. 3b). A few cells also formed air sacs with the expression of type I pneumocyte markers PDPN (Fig. 3c, d), HOPX (Fig. 3e), and AQP5 (Fig. 3f) 14 days after transplantation. Taken together, these findings demonstrate that mDASCs could incorporate in the damaged lung and differentiated into type I pneumocyte cells which were contributory to the repair process.

Interestingly, we found no incorporation of mDASCs when they transplanted into the normal lung (Additional file 2: Figure S2b), the weight changes (Additional file 2: Figure S2c), and lung wet/dry ratios (Additional file 2: Figure S2d) of mice showed that mDASCs had no effect on normal lungs, which was

confirmed by tissue histology (Additional file 2: Figure S2e). We also transplanted the basal cells isolated from the mouse cervix epithelium to the lung 7 days after bleomycin injury as a control to determine the paracrine effect of mDASCs. However, we did not find their incorporation in the injured lungs 7 days after transplantation (Additional file 2: Figure S2f). These data indicated the special incorporation ability of mDASCs in damaged lung.

Transplanted mDASCs decreased the pulmonary fibrosis in a bleomycin mouse model

To determine how mDASCs affect pulmonary fibrogenesis, the extent of pulmonary fibrosis was analyzed.

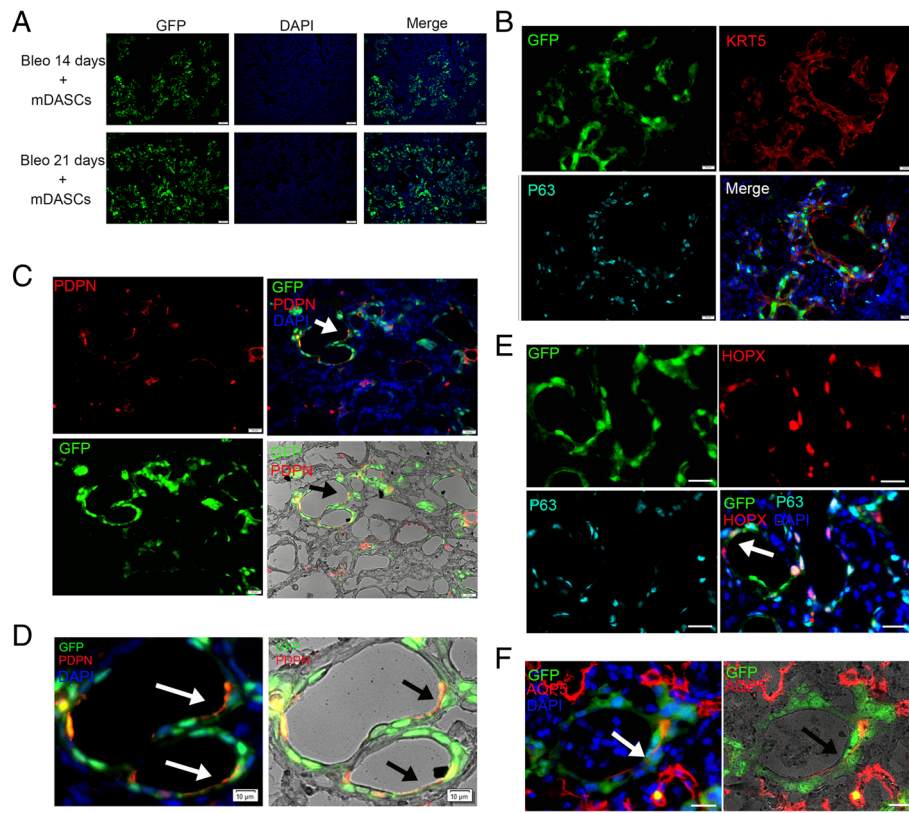


Fig. 3 Transplanted mDASCs incorporated in damaged lung and differentiated into type I pneumocytes. **a** Distribution of transplanted GFP-labeled cells in lung parenchyma by direct fluorescence. Scale bar, 50 μ m. **b** Immunostaining of GFP-labeled mDASCs with anti-GFP, anti-KRT5, and anti-P63 antibodies 7 days after transplantation. Scale bar, 20 μ m. **c** Immunostaining of transplanted GFP-labeled mDASCs in the lung parenchyma with anti-GFP and anti-PDPN (type I alveolar cell marker) antibodies 14 days after transplantation. Scale bar, 20 μ m. **d** Amplification inset in **c** indicates a regenerated alveolar structure. Scale bar, 10 μ m. **e** Immunostaining of transplanted GFP-labeled mDASCs in the lung parenchyma with anti-GFP, anti-HOPX (type I alveolar cell marker), and anti-P63 antibodies 14 days after transplantation. Scale bar, 20 μ m. **f** Immunostaining of transplanted GFP-labeled mDASCs in the lung parenchyma with anti-GFP and anti-AQP5 (type I alveolar cell marker) antibodies 14 days after transplantation. Scale bar, 20 μ m. Arrows show the co-localization staining of GFP and indicated marker

Representative microphotographs of H&E staining are shown in Fig. 4a. In the control groups, lung tissues showed a normal structure and clear pulmonary alveoli. Seven days after bleomycin administration, the lung tissue displayed obvious inflammatory cell infiltration, vascular congestion, thickened septa, and alveolar collapse. Fibrosis is fully developed with extensive and diffuse involvement of the lung at 21 days. In contrast, pulmonary fibrosis tended to decrease and the lesions were significantly attenuated when administered with mDASCs (Fig. 4b). Masson's trichrome staining of lung tissue (Fig. 4c) showed that more prominent blue staining, which represents mature collagen, was distributed in the alveolar septa or interstitial and peribronchial connective tissue in the bleomycin-injured lung without mDASC transplantation than that in the lung with mDASC transplantation (Fig. 4d). These findings support that engraftment of mDASCs 7 days after bleomycin instillation protected pulmonary fibrosis on days 14 and 21.

We also examined the content of hydroxyproline, a major constituent of collagen in the lung tissues (Fig. 5a). Compared with the control group, hydroxyproline content of the lung significantly increased in the bleomycin-treated group. However, administration of mDASCs significantly inhibited the hydroxyproline accumulation induced by bleomycin. Accumulation of α -SMA is a hallmark of pathological remodeling in pulmonary fibrosis, so the expression of α -SMA protein was examined at different time points by Western blotting (Fig. 5b, c) and immunofluorescence (Fig. 5d). After bleomycin instillation, acute lung inflammation developed (day 7), and at this stage, we observed no change of α -SMA expression compared with the control group, but the expression of α -SMA increased following bleomycin treatment in lung tissues on days 14 and 21, which were significantly alleviated by treatment with mDASCs.

To determine if the observed effect of mDASCs was associated with secreted factors, we assessed the ability of the conditioned medium (CM) of mDASCs to inhibit

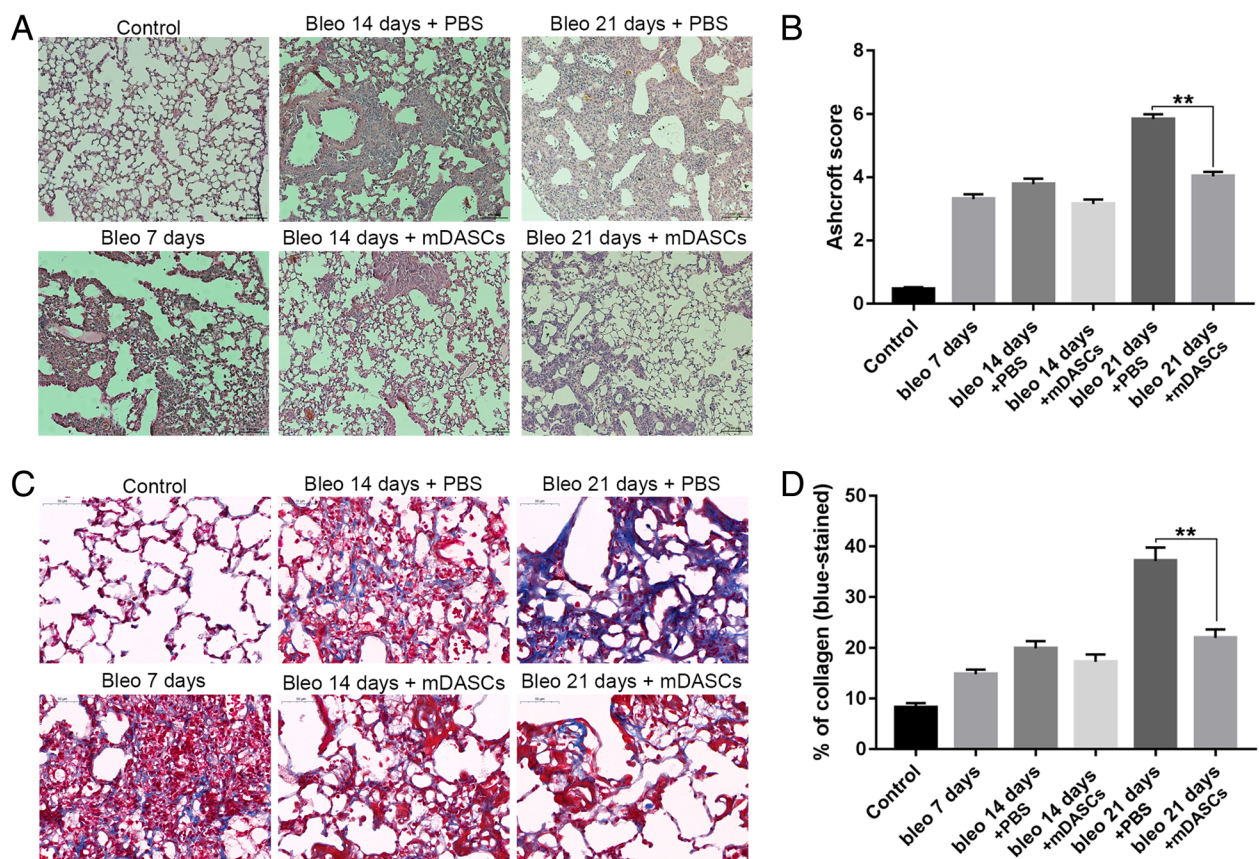


Fig. 4 The protective effect of transplanted mDASCs on bleomycin-induced pulmonary fibrosis development. **a** The mDASCs were transplanted into recipient mice 7 days after bleomycin instillation, and the lung sections were stained by hematoxylin and eosin (H&E) 7, 14, and 21 days after bleomycin instillation. Scale bar, 100 μ m. **b** Ashcroft score of lung fibrosis for panel **a**. $n = 4$. Error bars, S.E.M. $**P < 0.01$. **c** Using the same experimental setting, the lung sections were stained by Masson's trichrome for collagen I deposition (blue). Scale bar, 50 μ m. **d** Quantitation of the collagen content for panel **b**. $n = 5$. Error bars, S.E.M. $**P < 0.01$

hydroxyproline accumulation by intratracheally instilling with 30 μ l CM 7 days after bleomycin injury, and the hydroxyproline content was measured 14 days after administration of CM. There was no significant effect of CM from mDASCs on hydroxyproline content in comparison with the control medium (with no cell) (Additional file 2: Figure S2 g).

Transplanted mDASCs improved pulmonary function in bleomycin-induced pulmonary fibrosis mice

As presented in Fig. 6, bleomycin instillation markedly reduced O_2 saturation and O_2 partial pressure while it increased CO_2 partial pressure in arterial blood in 7, 14, and 21 days. In contrast, the mice administrated with mDASCs demonstrated healthier post-injury pulmonary function as shown by the higher O_2 saturation and O_2 partial pressure, yet lower CO_2 partial pressure. The data above showed that the mDASC transplantation could protect mouse lung and improve the pulmonary function of the recipients.

The protective effect of transplanted mDASCs on bleomycin-induced mortality in mice

To evaluate the protective effect of mDASCs on bleomycin-injured mice, animals were given a lethal dose of bleomycin (5 U/kg) on day 0 and mDASCs (1×10^6 in the volume of 30 μ l) or the same volume of PBS was instilled into the lung on day 7. As shown in Fig. 7a, mice began to die 9 days after the administration of bleomycin; the accumulative mortalities during 24 days were 40% in mDASC treatment groups, which were significantly lower than those in PBS administration groups (67%). Mice administrated with mDASCs could survive over 40 days, although mDASCs had no significant effects on the body weight of bleomycin-injured mice (Fig. 7b). These data indicated that mDASCs could significantly reduce bleomycin-induced mortality in mice.

Discussion

The present study firstly demonstrated that the transplantation of mDASCs at the acute injury stage could ameliorate the following fibrosis, improve lung function,

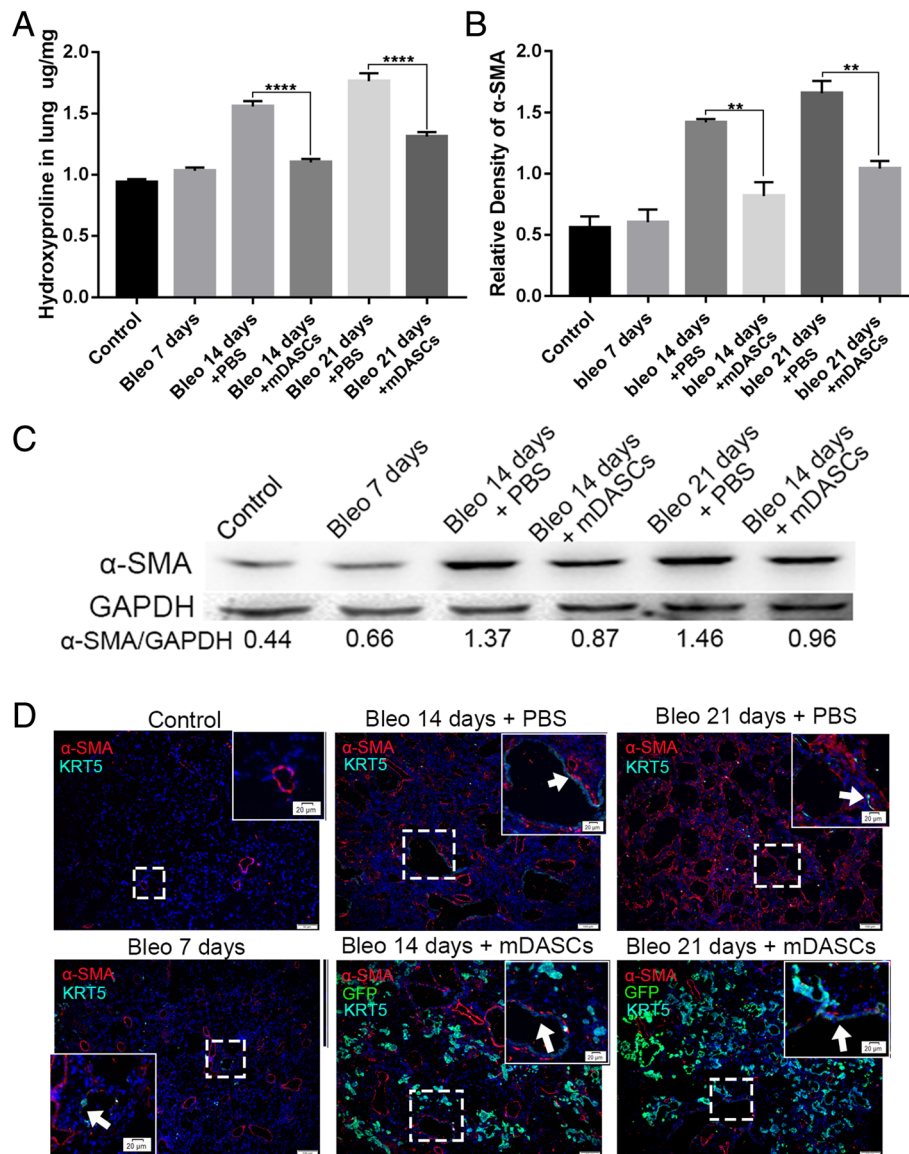
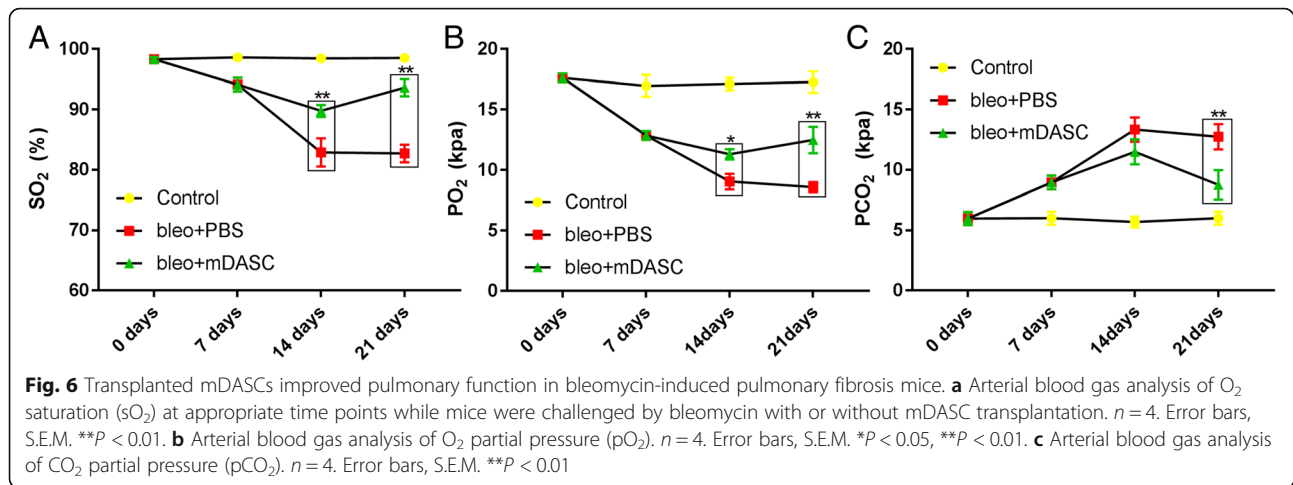


Fig. 5 Transplanted mDASCs decreased the collagen content and expression of α-SMA in lungs in bleomycin-induced pulmonary fibrosis mice. **a** Collagen deposition was assessed by measuring the hydroxyproline content in lung tissue. $n = 5$. Error bars, S.E.M. $^{***}P < 0.01$. **b, c** Western blotting of α-SMA expression and its quantification in lung tissues challenged by bleomycin with or without mDASC treatment. Samples were obtained at 7, 14, and 21 day after bleomycin exposure. $n = 3$. Error bars, S.E.M. $^{**}P < 0.01$. **d** Immunofluorescence of α-SMA in a lung section 7, 14, and 21 days after bleomycin exposure treated with or without mDASCs. Scale bar, 50 μm. The endogenous mDASCs are indicated by arrows. Scale bar, 50 μm and 20 μm in amplification inset

and reduce mortality in bleomycin-induced fibrosis mice. Therefore, DASCs could be an ideal candidate stem cell for the therapy of pulmonary fibrosis.

Tissue-specific stem cells have been identified as multipotent cells with the capacity for long-term self-renewal and the ability to differentiate into other cell lineages. These stem cells are typically quiescent in normal conditions and proliferate during injury repair [19–21]. Endogenous adult lung stem cells are important for epithelial cell homeostasis and injury repair which have

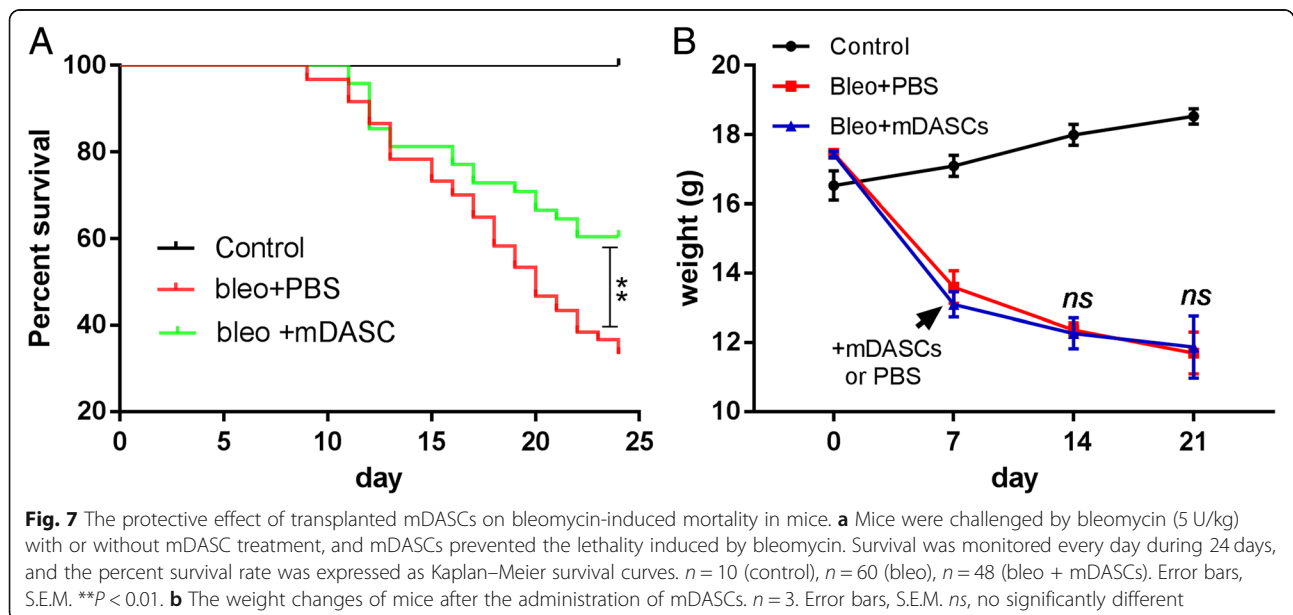
attracted significant interest. Numerous studies of human and animal lung have identified subsets of lung epithelial cells that could respond to lung injury with self-renewal and differentiation capacity, including basal cells, club cells, and AECII cells of the alveoli [12, 22, 23]. Moreover, advanced lineage tracing techniques have suggested that most types of lung epithelial cells can proliferate and expand after injury to promote lung repair [24–28]. Several studies demonstrated that P63+/KRT5+ mDASCs underwent rapid proliferation and migration to damaged



alveolar regions in response to influenza-induced ARDS. These migrated cells assembled and expressed typical alveoli-associated markers which suggested that mDASCs played a role as an intermediate in the reconstitution of the alveolar-capillary network eradicated by viral infection [13–15].

A previous study reported that human KRT5+ basal cells were frequent in IPF distal lungs compared with healthy lungs and these basal cells expressed differentiated epithelial cell markers, indicating that they were likely attempting to regenerate the epithelium [29]. As expected, we observed the proliferating endogenous mDASCs^{p63/Krt5} in the damage lung in bleomycin-induced lung injury mice, which were hard to find in the healthy lung.

Different animal models have been developed to investigate key mechanisms underlying pathogenesis of pulmonary fibrosis and identify potential therapeutic targets. The most common pulmonary fibrosis model involves exposure to bleomycin, and several studies reported that administration of bleomycin to the lung causes pulmonary injury and inflammation, and then a chronic fibrotic process develops [30–32], which is characterized by replacement of extracellular matrix by fibrillar collagen and collagen-producing myofibroblasts [33]. Our findings showed that bleomycin induced a significant acute lung injury in 7 days and then caused obvious fibrosis in day 21. Therefore, these findings were consistent with the previous studies. The mDASCs were applied in the acute injury stage.



In our experiments, we observed large-scale incorporation of transplanted mDASCs into mouse lung. The engrafted mDASCs differentiated into alveolar-like structure in 21 days, and a fraction of them expressed type I pneumocyte markers but not the type II pneumocyte marker. However, Zuo et al. reported that mDASCs expressed type I and type II pneumocyte markers 40 days after virus infection [15], and Vaughan et al. also found that ~ 1/3 of the Krt5+ cells resolved into type II pneumocytes 50 days after bleomycin injury [14]. The difference of differentiation time of transplanted mDASCs in animals between our experiment and theirs maybe the main cause. Together, these findings demonstrated that the mDASCs could incorporate, proliferate, and differentiate into type I pneumocyte cells which indicated the participation of regeneration and reparation following lung injury.

Furthermore, our results showed that administration of mDASCs 7 days after bleomycin instillation ameliorated the histopathological characteristics of lung tissues and prevented pulmonary fibrosis development. We therefore explored the underlying mechanism of the protective effect of mDASCs against pulmonary fibrosis caused by bleomycin. Hydroxyproline is a precursor of collagen, a key amino acid of collagen synthesis in the fibrotic lesions of mice. Compared to the control group, the injury group exhibited an obvious enhancement of hydroxyproline levels in lung tissues over time, consistent with previous studies [34, 35]. However, the treatment with mDASCs significantly decreased the hydroxyproline content in lung tissues. The development of bleomycin-induced pulmonary fibrosis was also related to the accumulation of α -SMA, which is a marker of myofibroblasts [36]. After bleomycin instillation, acute lung inflammation developed (day 7), and at this stage, we observed no change of α -SMA expression compared with the control group, but the expression of α -SMA increased on days 14 and 21, which were significantly alleviated by treatment with mDASCs.

In our study, bleomycin instillation markedly reduced O_2 saturation and O_2 partial pressure while it increased CO_2 partial pressure in arterial blood on days 7, 14, and 21. However, the administration of mDASCs helped mice recover to a healthier post-injury pulmonary function with higher O_2 saturation and O_2 partial pressure, yet lower CO_2 partial pressure. Consistent with this apparent protective effect in pulmonary function, the mDASCs improved the survival rates of mice injured by bleomycin.

We cannot exclude that the effects of mDASCs were indirect via induction of other molecules in the progression of fibrosis. For instance, the mDASCs exerted immunomodulatory effects that might influence CD45+ inflammatory cell infiltration in lung [14, 15]. Therefore, the mDASCs may play multiple roles (regeneration and/or immunomodulatory) in the progression of

fibrosis and the specific mechanism remains an area of intense study.

Conclusions

In summary, the mDASCs could ameliorate fibrosis, improve lung function, and reduce mortality of mice caused by bleomycin. This lung-protective effect is due to its process of lung regeneration and prevention of pulmonary fibrosis development. Therefore, DASCs may be a promising treatment for lung fibrosis.

Additional files

Additional file 1: Figure S1. a Anti-KRT5 and anti-P63 immunofluorescence staining of lung section 7 and 21 days after administration of PBS. b Negative control of immunofluorescence staining. The lung section was stained by secondary antibodies without primary antibodies 7 and 21 days after administration of bleomycin. Scale bar, 20 μ m. c Anti-KRT5 and anti-KI67 immunofluorescence staining of lung section 7 and 21 days after administration of PBS. Scale bar, 20 μ m. (TIF 16715 kb)

Additional file 2: Figure S2. a Anti-GFP and anti-KRT5 immunofluorescence staining of lung section 21 days after bleomycin exposure treated with or without mDASCs. Scale bar, 100 μ m. b Bright-field and direct fluorescence image of lungs from normal mice 7 days after transplantation of 1×10^6 GFP-labeled mDASCs. c The weight changes of normal mice after transplantation of mDASCs. $n = 3$. Error bars, S.E.M. *ns*, not significantly different. d The lung wet-to-dry weight ratios of normal mice after transplantation of mDASCs. $n = 3$. Error bars, S.E.M. *ns*, no significantly different. e Lung sections from normal mice were stained by hematoxylin and eosin (H&E) 7 days after transplantation of 1×10^6 GFP-labeled mDASCs. Scale bar, 200 μ m. f Bright-field and direct fluorescence image of lungs 6 h (left) and 7 days (right) after transplantation of 1×10^6 GFP-labeled mouse cervix basal cells or mDASCs. g The hydroxyproline content in the lung when mice were administrated by conditioned medium (CM) from mDASCs or control medium (with no cell) for 14 days after bleomycin injury. $n = 3$. Error bars, S.E.M. *ns*, no significantly different. (TIF 13826 kb)

Abbreviations

DASCs: Distal airway stem/progenitor cells; IPF: Idiopathic pulmonary fibrosis; KRT5: Keratin-5; pCO_2 : CO_2 partial pressure; pO_2 : O_2 partial pressure; sO_2 : O_2 saturation; W/D: Wet-to-dry weight

Acknowledgements

Not applicable.

Funding

This work was supported by National Natural Science Foundation of China (81570067, 81741104, 81570091, 81571822), Technology Innovation Project Ministry of Shanxi (712273033019), National Key Research Program(2017YFA0104600), Science and Scientific Research Initiation Funds for the Doctoral Program of Xi'an International University (XAIU2018070106).

Availability of data and materials

The datasets supporting the conclusions of this article are included within the article.

Authors' contributions

YS and MD designed and performed the experiments and wrote the paper. FJ and WZ supervised the research. YZ, WL, YG, and LH assisted with the experiments. MC and HL assisted with the data analysis. All authors discussed the results and commented on the manuscript. All authors read and approved the final manuscript.

Ethics approval and consent to participate

All procedures were conducted with the approval of the ethics committee of the Fourth Military Medical University and in accordance with the Institutional Animal Care and Use Committee of the Fourth Military Medical University. The mDASC cell line was generated and published by our group (Zuo et al., *Nature*, 2015).

Consent for publication

Not applicable.

Competing interests

The authors declare that they have no competing interests.

Publisher's Note

Springer Nature remains neutral with regard to jurisdictional claims in published maps and institutional affiliations.

Author details

¹Department of Respiratory and Critical Care Medicine, Tangdu Hospital, Fourth Military Medical University, Xi'an 710038, People's Republic of China.

²Xi'an International University, Xi'an 710077, People's Republic of China.

³Shanghai East Hospital, School of Medicine, Tongji University, Shanghai 200120, People's Republic of China. ⁴Kiangnan Stem Cell Institute, Zhejiang 311300, People's Republic of China. ⁵Ningxia Medical University, Yinchuan 750004, People's Republic of China.

Received: 25 January 2019 Revised: 24 April 2019

Accepted: 8 May 2019 Published online: 03 June 2019

References

- Gross TJ, Hunninghake GW. Idiopathic pulmonary fibrosis. *N Engl J Med*. 2001;345(7):517–25 PubMed PMID: 11519507.
- Phan SH. Fibroblast phenotypes in pulmonary fibrosis. *Am J Respir Cell Mol Biol*. 2003;29(3 Suppl):S87–92 PubMed PMID: 14503563.
- Hinz B, Phan SH, Thannickal VJ, Galli A, Bochaton-Piallat ML, Gabbiani G. The myofibroblast: one function, multiple origins. *Am J Pathol*. 2007;170(6):1807–16 PubMed PMID: 17525249. Pubmed Central PMCID: 1899462.
- Castriotta RJ, Eldadah BA, Foster WM, Halter JB, Hazzard WR, Kiley JP, et al. Workshop on idiopathic pulmonary fibrosis in older adults. *Chest*. 2010;138(3):693–703 PubMed PMID: 20822991. Pubmed Central PMCID: 4694103.
- Raghu G, Rochwerf B, Zhang Y, Garcia CA, Azuma A, Behr J, et al. An official ATS/ERS/JRS/ALAT clinical practice guideline: treatment of idiopathic pulmonary fibrosis. An update of the 2011 clinical practice guideline. *Am J Respir Crit Care Med*. 2015;192(2):e3–19 PubMed PMID: 26177183.
- Gurtner GC, Werner S, Barrandon Y, Longaker MT. Wound repair and regeneration. *Nature*. 2008;453(7193):314–21 PubMed PMID: 18480812.
- King RS, Newmark PA. The cell biology of regeneration. *J Cell Biol*. 2012;196(5):553–62 PubMed PMID: 22391035. Pubmed Central PMCID: 3307701.
- Clevers H. The intestinal crypt, a prototype stem cell compartment. *Cell*. 2013;154(2):274–84 PubMed PMID: 23870119.
- Tanimizu N, Mitaka T. Re-evaluation of liver stem/progenitor cells. *Organogenesis*. 2014;10(2):208–15 PubMed PMID: 24451175. Pubmed Central PMCID: 4154955.
- Huang J, Zhao X, Wang J, Cheng Y, Wu Q, Wang B, et al. Distinct roles of Dlk1 isoforms in bi-potential differentiation of hepatic stem cells. *Stem Cell Res Ther*. 2019;10(1):31 PubMed PMID: 30646961. Pubmed Central PMCID: 6334473.
- Hogan BL, Barkauskas CE, Chapman HA, Epstein JA, Jain R, Hsia CC, et al. Repair and regeneration of the respiratory system: complexity, plasticity, and mechanisms of lung stem cell function. *Cell Stem Cell*. 2014;15(2):123–38 PubMed PMID: 25105578. Pubmed Central PMCID: 4212493.
- Kotton DN, Morrissey EE. Lung regeneration: mechanisms, applications and emerging stem cell populations. *Nat Med*. 2014;20(8):822–32 PubMed PMID: 25100528. Pubmed Central PMCID: 4229034.
- Kumar PA, Hu Y, Yamamoto Y, Hye NB, Wei TS, Mu D, et al. Distal airway stem cells yield alveoli in vitro and during lung regeneration following H1N1 influenza infection. *Cell*. 2011;147(3):525–38 PubMed PMID: 22036562. Pubmed Central PMCID: 4040224.
- Vaughan AE, Brumwell AN, Xi Y, Gotts JE, Brownfield DG, Treutlein B, et al. Lineage-negative progenitors mobilize to regenerate lung epithelium after major injury. *Nature*. 2015;517(7536):621–5 PubMed PMID: 25533958. Pubmed Central PMCID: 4312207.
- Zuo W, Zhang T, Wu DZ, Guan SP, Liew AA, Yamamoto Y, et al. p63(+)Krt5(+) distal airway stem cells are essential for lung regeneration. *Nature*. 2015;517(7536):616–20 PubMed PMID: 25383540.
- Yang Y, Riccio P, Schotsaert M, Mori M, Lu J, Lee DK, et al. Spatial-temporal lineage restrictions of embryonic p63(+) progenitors establish distinct stem cell pools in adult airways. *Dev Cell*. 2018;44(6):752–61 e4 PubMed PMID: 29587145. Pubmed Central PMCID: 5875454.
- Imai-Matsushima A, Martin-Sancho L, Karlas A, Imai S, Zoranovic T, Hocke AC, et al. Long-term culture of distal airway epithelial cells allows differentiation towards alveolar epithelial cells suited for influenza virus studies. *EBioMedicine*. 2018;33:230–41 PubMed PMID: 29937069. Pubmed Central PMCID: 6085545.
- Ashcroft T, Simpson JM, Timbrell V. Simple method of estimating severity of pulmonary fibrosis on a numerical scale. *J Clin Pathol*. 1988;41(4):467–70 PubMed PMID: 3366935. Pubmed Central PMCID: 1141479.
- Potten CS, Loeffler M. Stem cells: attributes, cycles, spirals, pitfalls and uncertainties. Lessons for and from the crypt. *Development*. 1990;110(4):1001–20 PubMed PMID: 2100251.
- Kolios G, Moodley Y. Introduction to stem cells and regenerative medicine. *Respiration*. 2013;85(1):3–10 PubMed PMID: 23257690.
- Leeman KT, Fillmore CM, Kim CF. Lung stem and progenitor cells in tissue homeostasis and disease. *Curr Top Dev Biol*. 2014;107:207–33 PubMed PMID: 24439808. Pubmed Central PMCID: 4038302.
- Evans MJ, Dekker NP, Cabral-Anderson LJ, Freeman G. Quantitation of damage to the alveolar epithelium by means of type 2 cell proliferation. *Am Rev Respir Dis*. 1978;118(4):787–90 PubMed PMID: 707897.
- Adamson IY, Bowden DH. Origin of ciliated alveolar epithelial cells in bleomycin-induced lung injury. *Am J Pathol*. 1977;87(3):569–80 PubMed PMID: 68683. Pubmed Central PMCID: 2032137.
- Rawlins EL, Hogan BL. Epithelial stem cells of the lung: privileged few or opportunities for many? *Development*. 2006;133(13):2455–65 PubMed PMID: 16735479.
- Rawlins EL, Ostrowski LE, Randell SH, Hogan BL. Lung development and repair: contribution of the ciliated lineage. *Proc Natl Acad Sci U S A*. 2007;104(2):410–7 PubMed PMID: 17194755. Pubmed Central PMCID: 1752191.
- Rawlins EL, Hogan BL. Ciliated epithelial cell lifespan in the mouse trachea and lung. *Am J Physiol Lung Cell Mol Physiol*. 2008;295(1):L231–4 PubMed PMID: 18487354. Pubmed Central PMCID: 2494792.
- Rawlins EL, Okubo T, Que J, Xue Y, Clark C, Luo X, et al. Epithelial stem/progenitor cells in lung postnatal growth, maintenance, and repair. *Cold Spring Harb Symp Quant Biol*. 2008;73:291–5 PubMed PMID: 19028985.
- Borthwick DW, Shahbazian M, Krantz QT, Dorin JR, Randell SH. Evidence for stem-cell niches in the tracheal epithelium. *Am J Respir Cell Mol Biol*. 2001;24(6):662–70 PubMed PMID: 11415930.
- Smirnova NF, Schamberger AC, Nayakanti S, Hatz R, Behr J, Eickelberg O. Detection and quantification of epithelial progenitor cell populations in human healthy and IPF lungs. *Respir Res*. 2016;17(1):83 PubMed PMID: 27423691. Pubmed Central PMCID: 4947297.
- Moore BB, Hogaboam CM. Murine models of pulmonary fibrosis. *Am J Physiol Lung Cell Mol Physiol*. 2008;294(2):L152–60 PubMed PMID: 17993587.
- Chaudhary NI, Schnapp A, Park JE. Pharmacologic differentiation of inflammation and fibrosis in the rat bleomycin model. *Am J Respir Crit Care Med*. 2006;173(7):769–76 PubMed PMID: 16415276.
- Limjunyawong N, Mitzner W, Horton MR. A mouse model of chronic idiopathic pulmonary fibrosis. *Physiol Rep*. 2014;2(2):e00249 PubMed PMID: 24744912. Pubmed Central PMCID: 3966254.
- Walters DM, Kleeberger SR. Mouse models of bleomycin-induced pulmonary fibrosis. *Curr Protoc Pharmacol*. 2008;Chapter 5(Unit 5):46 PubMed PMID: 22294226.
- Zhao L, Wang X, Chang Q, Xu J, Huang Y, Guo Q, et al. Neferine, a bisbenzylisoquinoline alkaloid attenuates bleomycin-induced pulmonary fibrosis. *Eur J Pharmacol*. 2010;627(1–3):304–12 PubMed PMID: 19909737.
- Arizmendi N, Puttagunta L, Chung KL, Davidson C, Rey-Parra J, Chao DV, et al. Rac2 is involved in bleomycin-induced lung inflammation leading to pulmonary fibrosis. *Respir Res*. 2014;15:71 PubMed PMID: 24970330. Pubmed Central PMCID: 4082672.
- Vyalov SL, Gabbiani G, Kapanci Y. Rat alveolar myofibroblasts acquire alpha-smooth muscle actin expression during bleomycin-induced pulmonary fibrosis. *Am J Pathol*. 1993;143(6):1754–65 PubMed PMID: 7504890. Pubmed Central PMCID: 1887256.